Adv Polym Sci (2017) 278: 99–126
DOI: 10.1007/12_2017_4

Published online: 10 May 2017

On-Surface Polymerization: From Polyarylenes to Graphene Nanoribbons and Two-Dimensional Networks

Matthias Koch, Stefan Hecht, and Leonhard Grill

Abstract On-surface polymerization is a novel technique for the fabrication of one- and two-dimensional molecular networks confined on a surface and is a rapidly developing field in surface science. The molecular building blocks exhibit pre-defined connection sites at which, after thermal activation and diffusion on the surface, the molecules are linked in a clean environment. Depending on the position and number of these connection sites, activated molecules polymerize to yield chains or two-dimensional networks. The chemical composition of the resulting polymer is precisely defined by the precursor molecules. We review current developments in the field of on-surface polymerization and present different examples, including the fabrication of graphene nanoribbons. We introduce reductive Ullmann-type coupling as well as Scholl-type cyclodehydrogenation for fabrication of graphene nanoribbons of increasing width. The surface plays a crucial role during the activation and polymerization processes because it serves as a catalyst, promotes molecular diffusion, and has a huge influence on the final molecular architecture. One-dimensional polymers can act as molecular wires and their conductance has been studied at the level of individual chains. In addition, we discuss two-dimensional networks and describe recent progress in attempts to improve their quality using sequential activation or defect-healing.

M. Koch
Department of Physical Chemistry, Fritz Haber Institute of the Max Planck Society, 14195 Berlin, Germany

S. Hecht
Department of Chemistry & IRIS Adlershof, Humboldt-Universität zu Berlin, 12489 Berlin, Germany

L. Grill (✉)
Department of Physical Chemistry, University of Graz, Heinrichstrasse 28, 8010 Graz, Austria
e-mail: leonhard.grill@uni-graz.at

Keywords Carbon-based materials • C–C coupling reactions • Molecular conductance • On-surface polymerization • On-surface synthesis • Scanning tunneling Microscopy • Step-growth polymerization • Surface chemistry • Surface science

Contents

On-surface polymerization is a recently developed bottom-up approach for the fabrication of one-dimensional polymer chains, including ladder-type polymers and ribbons, as well as two-dimensional sheets and networks. In many cases these structures are not accessible by solution synthesis or top-down fabrication [1]. The technique requires suitable monomers, typically (polycyclic) (hetero) aromatic building blocks, which react at specific predefined connection sites during the polymerization step. To prevent uncontrolled growth, the monomers need to be chemically inert and their reactivity unleashed only after an activation step. One particularly popular approach for this "turn on" reactivity is equipping the molecular building blocks with halogen substituents, which can readily be cleaved by heat, and stabilizing the formed carbon-based radicals on the underlying metal surface. The activated monomer can form covalent aryl–aryl bonds at these reactive sites, allowing fabrication of large macromolecules in a very well-defined manner and in an extremely clean environment. The absence of solvent means that there is no need to solubilize side chains. In contrast, deposition of macromolecules by conventional evaporation techniques in ultrahigh vacuum is difficult to achieve because the high temperatures required typically lead to decomposition.

1 On-Surface Polymerization by Dehalogenation

The process of on-surface polymerization can be separated into three subsequent steps: (1) deposition, when monomers, carrying halogen atoms to mask the desired reaction sites, are deposited onto the surface; (2) activation, when the halogen–carbon bonds are cleaved; and (3) coupling, when covalent bonds are formed

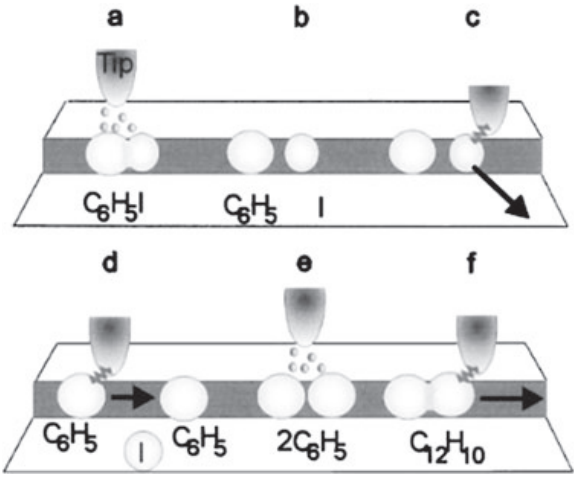

Fig. 1 Different synthesis steps induced by an STM tip: selective dissociation of the C–I bond in iodobenzene induced by electrons (**a, b**), lateral manipulation to remove the cleaved-off iodide (**c**), lateral manipulation to bring two phenyl moieties together (**d**), inelastic tunneling-induced phenyl–phenyl coupling (**e**), and lateral manipulation of the formed biphenyl to confirm successful reaction (**f**). Reproduced from [2]. Copyright (2000) by the American Physical Society

between activated monomers, leading to polymerization. As early as 2000, using iodobenzene molecules on Cu(111), Saw Hla et al. demonstrated each of these steps at the level of single molecules with the help of a low temperature scanning tunneling microscope (STM) (see Fig. 1) [2].

These experiments were performed at a temperature of 20 K to freeze the diffusion of iodobenzene molecules. By applying a bias pulse with the STM tip right on top of the molecule, dissociation of the iodine atom can be induced and a reactive phenyl radical, which is stabilized by interaction with the copper step edge, is generated. In the next step, lateral manipulation is used to move two of such reactive phenyl species next to each other. Finally, coupling of the two radicals is induced by another lower voltage pulse, which induces rotation and subsequently leads to formation of a covalent C–C bond in the biphenyl product, resembling an Ullmann-type coupling reaction [3] on the single molecule level. The beauty of this procedure is that each individual step of the reaction is induced by the STM tip and, hence, each intermediate stage can be studied. This pioneering work laid the foundation for what has become the field of on-surface polymerization.

Although this degree of control over a chemical process is more than sensational, the growth of large polymeric structures requires at least bifunctional building blocks (monomers) and automation of both activation and coupling reactions. For this, a constant stimulus is needed, supplying the activation energy for both processes. The most convenient form of energy to apply is heat in combination with the proper surface. An appropriate surface is crucial because it is much more than a template for performing the reaction and many studies have shown that the

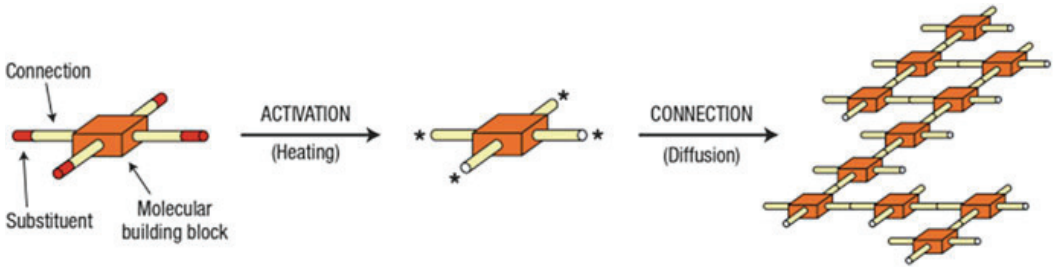

Fig. 2 Principle of the on-surface polymerization technique [1, 7]. Reproduced from [7]

choice of surface has a strong influence on the occurrence of the polymerization process and the resulting final product. For example, the activation energy required to dissociate a halogen atom and the mobility of the monomer and oligomer building blocks vary with the choice of substrate [4]. Thereby, not only the composition of the substrate (e.g,. Cu versus Ag versus Au) but also the surface reconstruction play important roles, specific sites sometimes displaying enhanced reactivity [5].

To automate polymerization, monomers are deposited on the surface and the molecules self-assemble in more or less extended two-dimensional (2D) islands, depending on the coverage. These monomers are, as in the experiment discussed before, equipped with (at least two) halogen atoms at defined sites. The monomer is designed such that the bond between the halogen atom and the molecular framework is the weakest bond in the overall system. For example, the average bond energies of C–C and C–H bonds present on such aromatic systems are between 85 and 103 kcal/mol, whereas the C–Br and C–I bonds have bond dissociation energies of only 68 kcal/mol and 51 kcal/mol, respectively [6]. Monomers can be activated either by evaporating them at a higher temperature or, alternatively and more reliably, by heating the substrate to an elevated temperature. In contrast to local STM-tip-induced activation, this global heating step simultaneously addresses all molecular building blocks adsorbed on the surface. The elevated temperature of the substrate furthermore promotes both diffusion of the monomers (and oligomeric intermediates) and provides the necessary activation energy for their coupling. Therefore, the right combination of surface and monomer structure, together with a properly chosen reaction temperature to provide the necessary thermal activation for the dissociation, diffusion, and coupling steps, indeed allows their automation and integration into a powerful and highly efficient on-surface polymerization scheme (Fig. 2) [1, 7].

Using these powerful techniques, architectural control can be achieved by judicious choice of the monomer structure, including both the number and kind of halogen atoms as well as their relative orientation. Two halogen atoms provide either one-dimensional (1D) chains or cycles, whereas three or more halogens lead to formation of 2D networks.

2 One-Dimensional Oligomers

In early work, Weiss and coworkers studied 1,4-diiodobenzene on Cu(111) and observed formation of so-called "protopolymers" [8]. Later, Rosei, Perepichka, and coworkers found that the same monomer on Cu(110) was readily activated by C–I bond cleavage, yet required additional heating to 500 K to trigger formation of the covalent C–C bonds to yield poly(*para*-phenylene) [9]. When changing from the strictly linear *para*-relationship of the two iodine substituents in the monomer to *meta* (i.e., 1,3-diiodobenzene), they found formation of both *transoid* poly(*meta*-phenylene) chains as well as hexameric cycles (Fig. 3).

If the monomer units are connected to each other by more than one bond, ladder polymers are formed. Using Ullmann-type couplings in this fashion, 1,4,5,8-tetrabromonaphthalene can be polymerized at 470 K on Au(111) to yield such ladder polymers, resembling the narrowest possible graphene nanoribbon (GNR) with armchair edges (Fig. 4) [10]. The authors could show that the Au-bridged metallosupramolecular polymer is an intermediate of the polymerization process; it could be observed at 400 K and underwent reductive elimination to the GNR at 470 K.

Obtaining GNRs with increased width using solely Ullmann-type couplings is limited by the efficiency of the reaction, in particular in adjacent positions on the zig-zag edge of acenes. To circumvent this issue, the groups of Müllen and Fasel developed a two-step procedure to first polymerize a suitable dihalogenated

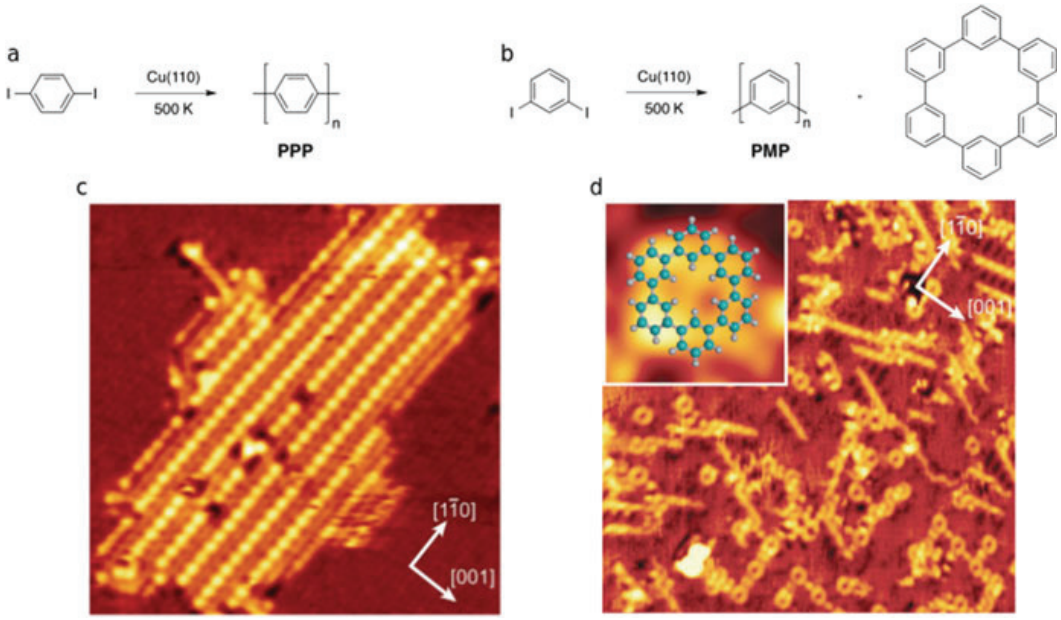

Fig. 3 On-surface polymerization on Cu(110) of either 1,4-diiodobenzene (**a**) or 1,3-diiodobenzene (**b**), resulting in formation of poly(*para*-phenylene) (PPP; **c**) and poly(*meta*-phenylene) (PMP) as well as hexameric macrocycles (**d**), respectively. Reproduced in part from [9]. Copyright (2009) by Wiley-VCH

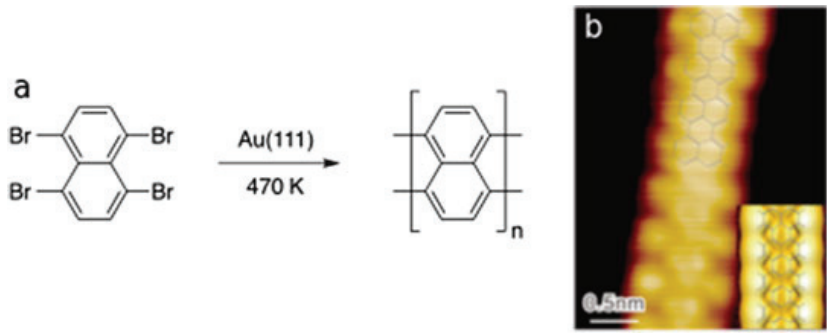

Fig. 4 Polymerization of 1,4,5,8-tetrabromonaphthalene (**a**) to yield narrow armchair graphene nanoribbons (**b**). Reproduced in part from [10]. Copyright (2015) American Chemical Society

monomer via single C–C bonds made with on-surface Ullmann-type coupling, followed by a second annealing step leading to cyclodehydrogenation, known in solution as the Scholl reaction [11]. This powerful route (Fig. 5) led to the successful bottom-up growth of armchair-edge GNRs from dibromodianthracene (DBDA) monomers [12]. After deposition on Au(111), the DBDA monomers arrange in large islands. Heating the substrate to 470 K cleaves the C–Br bonds, and anthracene oligomers (connected by C–C single bonds) are formed. In these oligomers/polymers, the neighboring anthracene units can be fused by a cyclodehydrogenation step, which is induced by increasing the temperature to 670 K.

For the formation of anthracene oligomers it is crucial that the DBDA monomers adsorb in a nonplanar twisted geometry on the Au(111) surface to minimize steric hindrance in the coupling step. This is in good agreement with a study using 9,10-dibromoanthracene (9,10-DBA), a single anthracene with two bromines in the opposing central *meso*-positions, which does not polymerize on Au(111) (Fig. 6) [13].

Even heating the substrate to 670 K does not lead to polymer formation; instead, desorption takes place. This finding is attributed to the planar adsorption geometry of 9,10-DBA and the associated steric hindrance of C–C coupling, whereas the approach of two twisted activated DBDA monomers is presumably associated with a much lower kinetic barrier.

The power of the on-surface polymerization strategy clearly lies in its inherent chemical precision. The structure of the resulting polymer on the surface is precisely determined by the monomer building blocks, in particular their symmetry and position of the reactive groups, which encode their connectivity. This has been beautifully demonstrated by the recent work of the Müllen and Fasel groups on the synthesis of various types of GNRs, in particular achieving precise control over edge structure, ranging from armchair (see Fig. 5) [12] all the way to zig-zag edges [14]. In the latter work, a cleverly designed monomer provided access to a

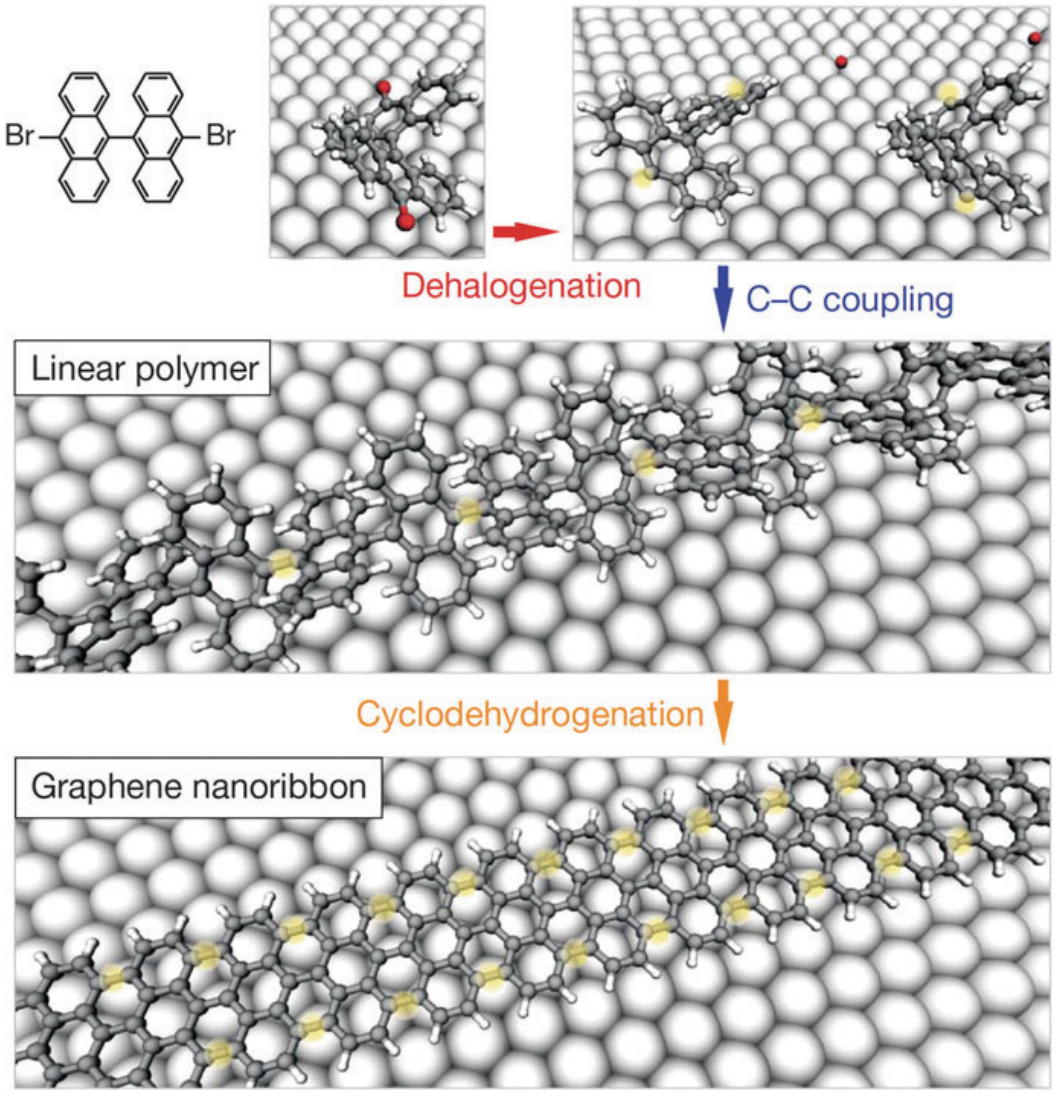

Fig. 5 On-surface polymerization of dibromodianthracene (DBDA) monomers to yield narrow armchair graphene nanoribbons. Reproduced from [12]. Copyright (2010) Nature Publishing Group

polyarylene precursor, which after subsequent cyclodehydrogenation yielded zig-zag edge GNRs of considerable width and length with atomic precision (Fig. 7).

In addition to the monomer structure, several other parameters should be considered in the design. For example, the monomers have to be sufficiently stable upon thermal treatment to enable their evaporation onto the surface under typically used UHV conditions at temperatures below the activation temperature.

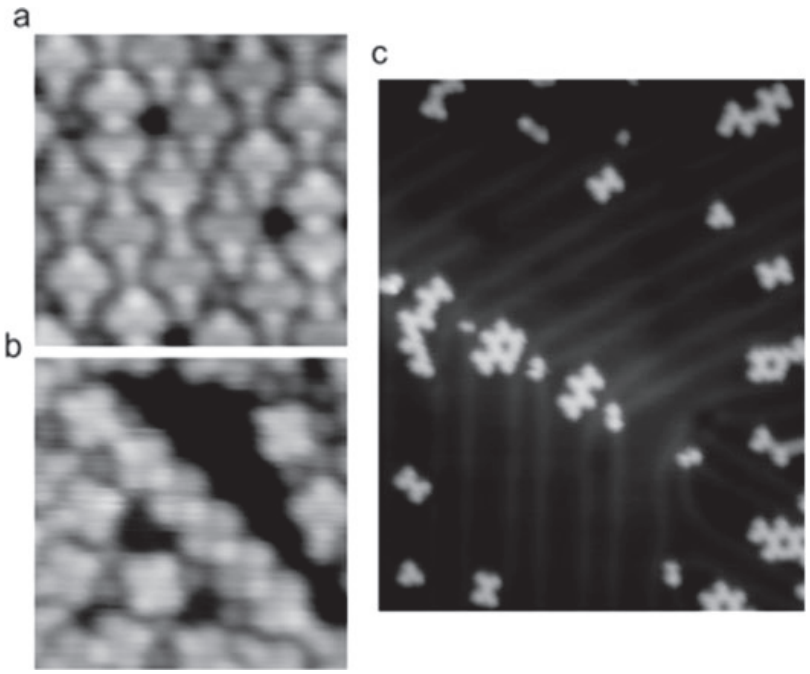

Fig. 6 Inhibited polymerization of 9,10-dibromoanthracene (9,10-DBA) on Au(111), presumably as a result of steric hindrance during coupling of planar activated monomers: 9,10-DBA on Au (111) before heating (**a**) and after heating the substrate to 470 K (**b**) and 670 K (**c**). Reproduced from [13]

3 Influence of the Surface

In addition to the molecular design criteria detailed above, the surface itself plays a decisive role during monomer activation and coupling (and potential annealing) and has a major influence on the occurrence and outcome of the on-surface polymerization process. As mentioned above, the surface can act as a catalyst for the initial activation step. Step edges, defects, and adatoms are highly reactive sites for promoting chemical reactions. At the same time, the surface stabilizes the formed radical species and enables diffusion of monomers. Reconstruction of the surface changes the binding energy and adsorption geometry. As discussed above, a larger binding energy can limit polymerization because of steric hindrance. Also, orientation of the monomers and the shape and size of the molecular networks and islands depends on the surface reconstruction.

We have studied 2,3-dibromoanthracene (2,3-DBA) on Au(111) and Au(100) surfaces (Fig. 8) [13]. The intact and nonactivated molecules arrange in a parallel manner on Au(111). This is in contrast to Au(100), where the molecules face each other. The appearance and length of a single 2,3-DBA molecule was similar on both surfaces, and to activate them the substrates were heated to 520 K.

On Au(111), the formation of narrow rod-like structures (Fig. 8d, e) and star-shaped molecules (Fig. 8g, h) has been observed. The rods appear to be dimers formed via a formal [2+2]cycloaddition, whereas the star-shaped molecules

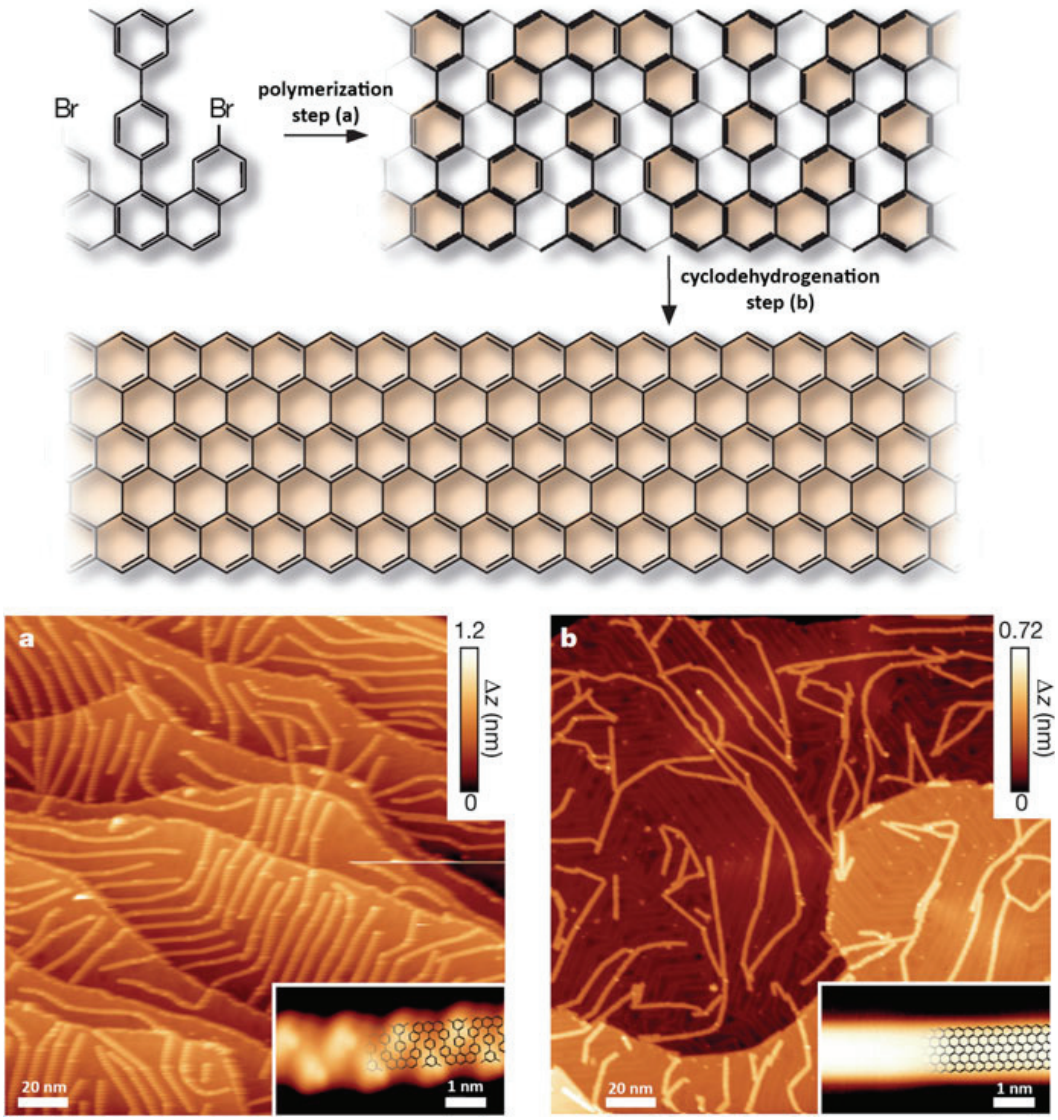

Fig. 7 On-surface polymerization of appropriately chosen monomer leads to formation of a polyarylene precursor (**a**), which after cyclodehydrogenation yields zig-zag edge graphene nanoribbons (**b**), sketched in the *upper panel*. Reproduced from [14]. Copyright (2016) Nature Publishing Group

resemble trimers arising from a [2+2+2]cycloaddition. In contrast, exclusively rod-like structures and no stars were formed on Au(100) (Fig. 8f). It appears that the parallel rows of the Au(100) surface favor dimerization in a head-to-head fashion, whereas the threefold symmetry on the Au(111) surface allows both dimerization and cyclotrimerization pathways.

In addition to the surface reconstruction, the type of metal substrate also plays an important role. This was exemplarily illustrated by a study of Cu(111), Ag(111), and Au(111) surfaces that suggested a different coupling probability for each surface [4]. In general, two effects oppose each other: activation by carbon–halogen dissociation is facilitated on the more reactive Cu(111) surface, but diffusion of the

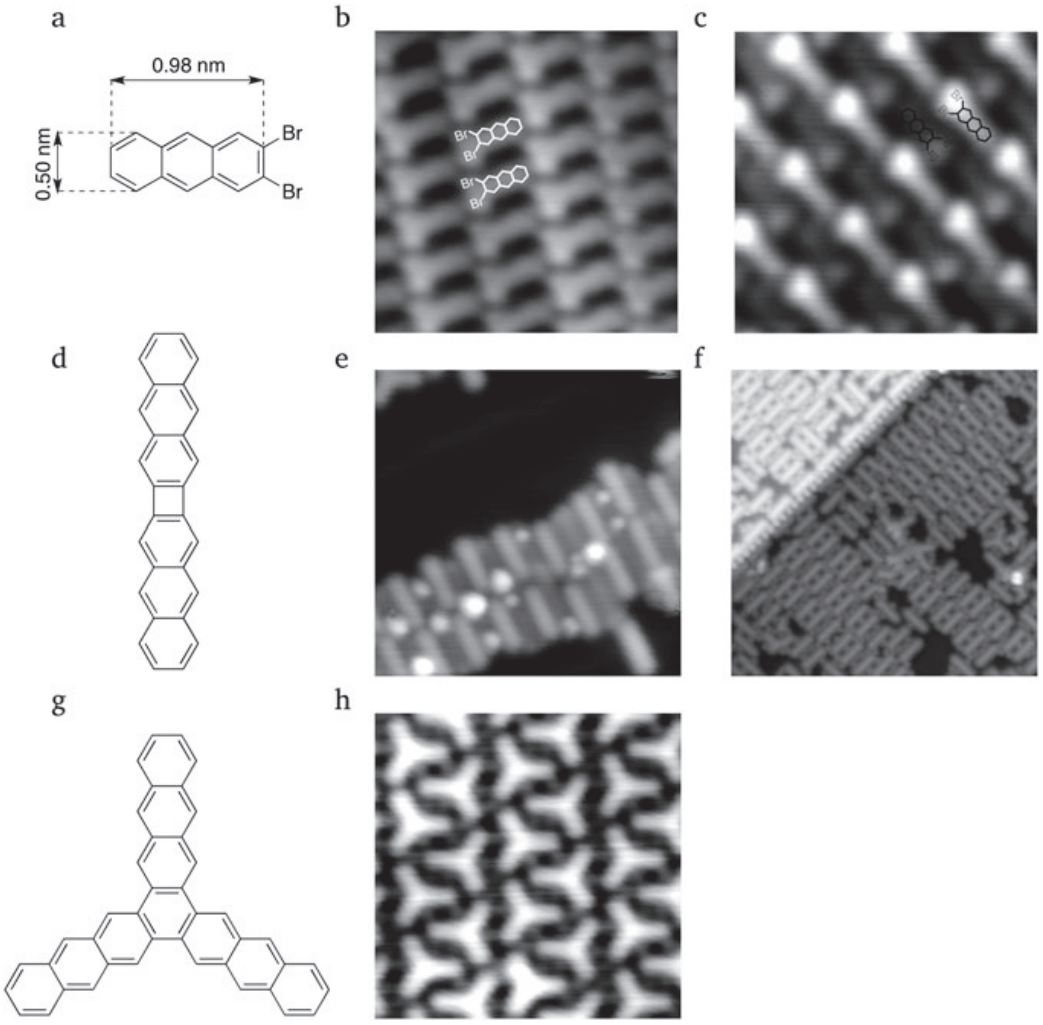

Fig. 8 Oligomerization of 2,3-dibromoanthracene (2,3-DBA) on Au(111) and Au(100). *Left*: 2,3-DBA monomer (**a**), observed linear dimer (**d**), and star-shaped trimer (**g**). *Center*: Intact tdDBA molecules adsorbed on Au(111) (**b**) and two species observed after heating the Au(111) sample (**e, h**). *Right*: Intact tdDBA molecules adsorbed on Au(100) (**c**) and species observed after heating the substrate (**f**). Reproduced from [13]

activated monomers and, hence, their coupling efficiency is decreased on the same surface. More specifically, Monte Carlo simulations showed that lower coupling probabilities lead to more closed networks, whereas higher coupling probability and lower mobility lead to branched network structures. Clearly, the choice of substrate is crucial for achieving efficient polymerization reactions and can dictate the resulting polymer architecture.

The fully aromatic framework of hexabenzocoronene (HBC), which can be considered as small graphene fragment, is known to adsorb in a flat and planar fashion on noble metal surfaces. The results of Soe et al. [15] suggest that the electronic states of two HBC molecules are able to hybridize, rendering HBC oligomers/polymers promising candidates for molecular wires (Fig. 9).

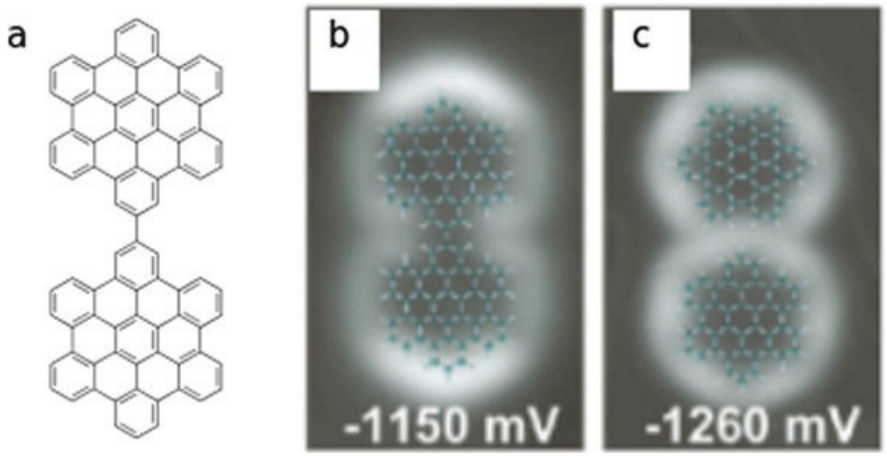

Fig. 9 Hexabenzocoronene dimer: chemical structure (**a**) and STM images at different bias voltages (**b, c**). Reproduced from [15]. Copyright (2012) American Chemical Society

In order to grow such molecular wires composed of linked HBC units, we investigated dibromohexabenzocoronene (DBHBC) equipped with two bromines in a *trans*-type relationship on Au(111) and Cu(111) surfaces [16]. Similar to the results of Walch and coworkers [17], we found that activation takes place at room temperature when depositing DBHBC onto a Cu(111) surface. The activation temperature depends strongly on the type of halogen but also on the substrate, as DBHBC is activated below room temperature on Cu(111), whereas a heating step to 520 K is required on Au(111). This can be explained by the higher catalytic reactivity of the Cu(111) substrate. The energy required to remove an atom from a Cu(111) step is lower than for Au(111), which results in more diffusing copper adatoms at room temperature, thus supporting the reaction. In accordance with the general trend that C–I bonds cleave at lower temperatures than C–Br bonds, as a result of lower bond dissociation energy, we found that diiodohexabenzocoronene (DIHBC) cleaves on Au(111) at 390 K. However, a much higher activation temperature is necessary in the absence of a catalytically active metal substrate. For example, on calcite ($CaCO_3$) cleavage of C–I bonds takes place only at temperatures above 570 K [18].

The bond that is formed between activated monomers depends on the substrate as well as temperature. On Au(111), a heating step to 520 K is required to activate the DBHBC precursor, leading to formation of covalent bonds between HBC monomers. In strong contrast, on Cu(111), activation occurs at room temperature and metal-coordination bonds are subsequently formed, connecting HBC monomers via Cu atoms (Fig. 10) [16].

Metal–carbon bonds are typically less stable than covalent C–C bonds but offer the advantage that the activation barrier associated with their formation is lower. This fact can be crucial for molecules that decompose at elevated temperatures, as illustrated by work on the assembly of molecular wagons [19]. On Cu(111), the formation of chains based on metal–carbon bonds is possible, but on Au(111) the required temperature for polymerization leads to decomposition of the molecules. Interestingly, during polymerization of tetrabromonaphthalene, gold–organic

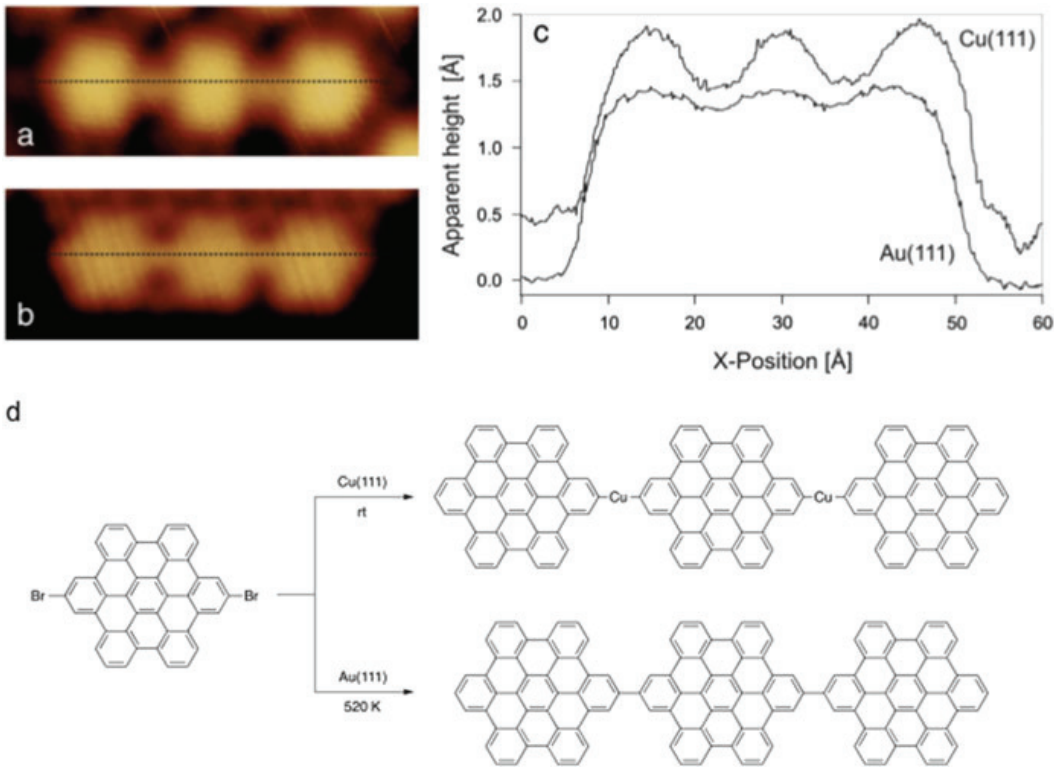

Fig. 10 Oligomerization of dibromohexabenzocoronene (DBHBC) on Cu(111) and Au(111): STM image of a HBC chain on Au(111) (**a**) and Cu(111) (**b**), including their height profiles (**c**). Chemical reaction pathways on Cu(111) and Au(111) (**d**). Reproduced from [16]

hybrids were observed if the sample was annealed below 470 K [10]. The formation of copper–organic hybrids is very common for Cu adatoms but has been rarely reported for Au. This intermediate stage, where Au-bridged metallosupramolecular polymers are formed, might be the reason why no products except GNRs are observed [10]. As a result of less stable Au–C linking, these bonds may be reversible and allow defect-healing to occur.

4 Doping of Molecular Chains

The electronic structure of $N = 7$ GNRs (N being the number of carbon atoms counted across the width of the GNR; see Fig. 5) has been characterized with scanning tunneling spectroscopy and other techniques [20–23]. The lowest unoccupied molecular orbital (LUMO) has been found at 1.6 eV and the highest occupied state (HOMO) at −1.1 eV on Au(111), leading to a HOMO–LUMO gap of 2.7 eV [20]. Both states are delocalized along the edges of the GNR. In addition to the HOMO and LUMO, an edge state located at the zig-zag edges of the GNR was observed close to the Fermi energy.

Different results have been reported for the band gap of chevron-shaped GNRs (Fig. 11). These GNRs have been fabricated with 6,11-dibromo-1,2,3,4-

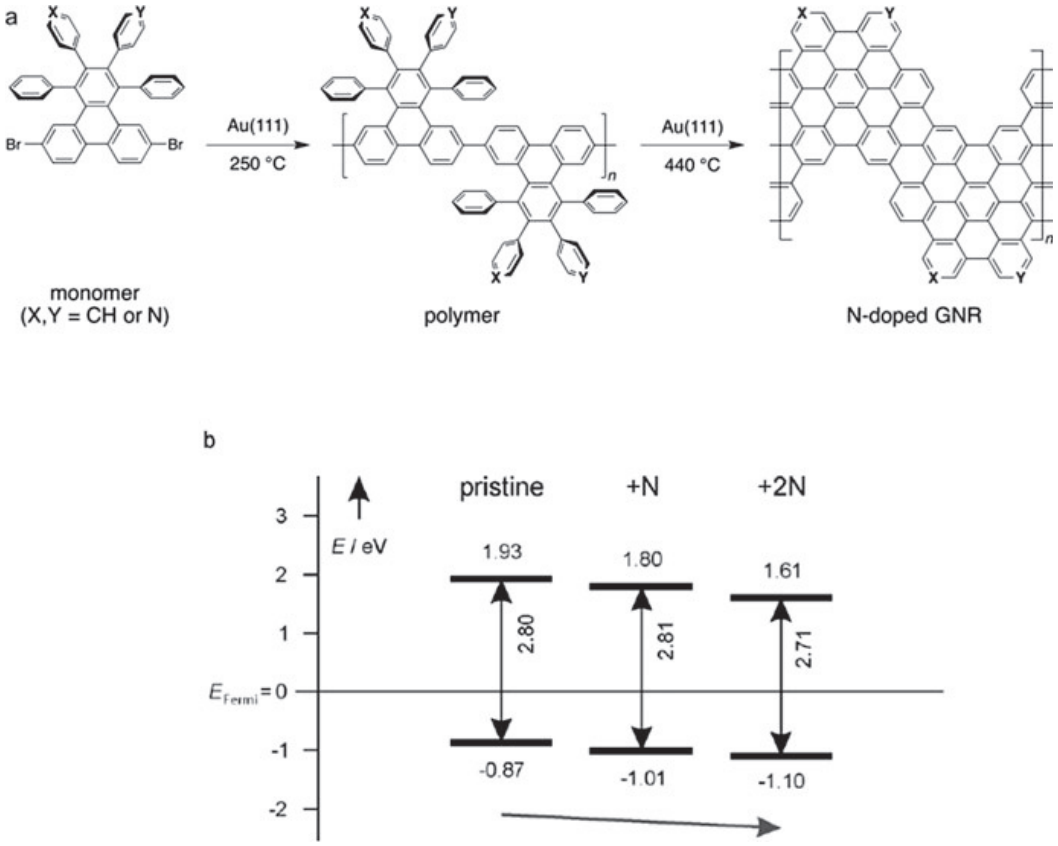

Fig. 11 Chevron-type GNRs with varying degree of n-doping in the armchair edge by on-surface polymerization of mono- and bispyridyl substituted monomers on Au(111) (**a**), showing that the band structure is shifted with each additional N atom (**b**). Reproduced in part from [25]. Copyright (2013) by Wiley-VCH

tetraphenyl-triphenylene as molecular building block [12, 24, 25]. Fasel et al. found a band gap of 2.0 eV [24], whereas high-resolution electron energy loss spectroscopy (HREELS) indicated a band gap of 2.8 eV [25].

The LUMO of pristine chevron-shaped nanoribbons is located at −0.87 eV. The ribbons are p-doped because of interaction with the Au(111) substrate [24]. By replacing carbon atoms in the precursor molecule it is possible to create GNRs with an atomically precise doping pattern [24, 25]. By exchanging one or two carbon atoms in the molecular building block with nitrogen, the entire band structure is shifted by 0.1 eV or 0.2 eV, respectively (see Fig. 11) [25]. Each nitrogen atom shifts the band structure by about 0.1 eV, whereas the band gap is only weakly influenced by n-doping. By mixing pristine 6,11-dibromo-1,2,3,4-tetraphenyl-triphenylene with n-doped 5,5′-(6,11-dibromo-1,4-diphenyl-triphenylene-2,3-diyl)dipyrimidine, p-N-GNR heterojunctions are formed. According to Fasel and coworkers, the band gap of ~2.0 eV is similar for both GNRs on Au(111) but the position of the valence band maximum of the p-doped pristine GNRs is closer to the Fermi level of the metallic substrate [24]. Local density of states (LDOS) maps

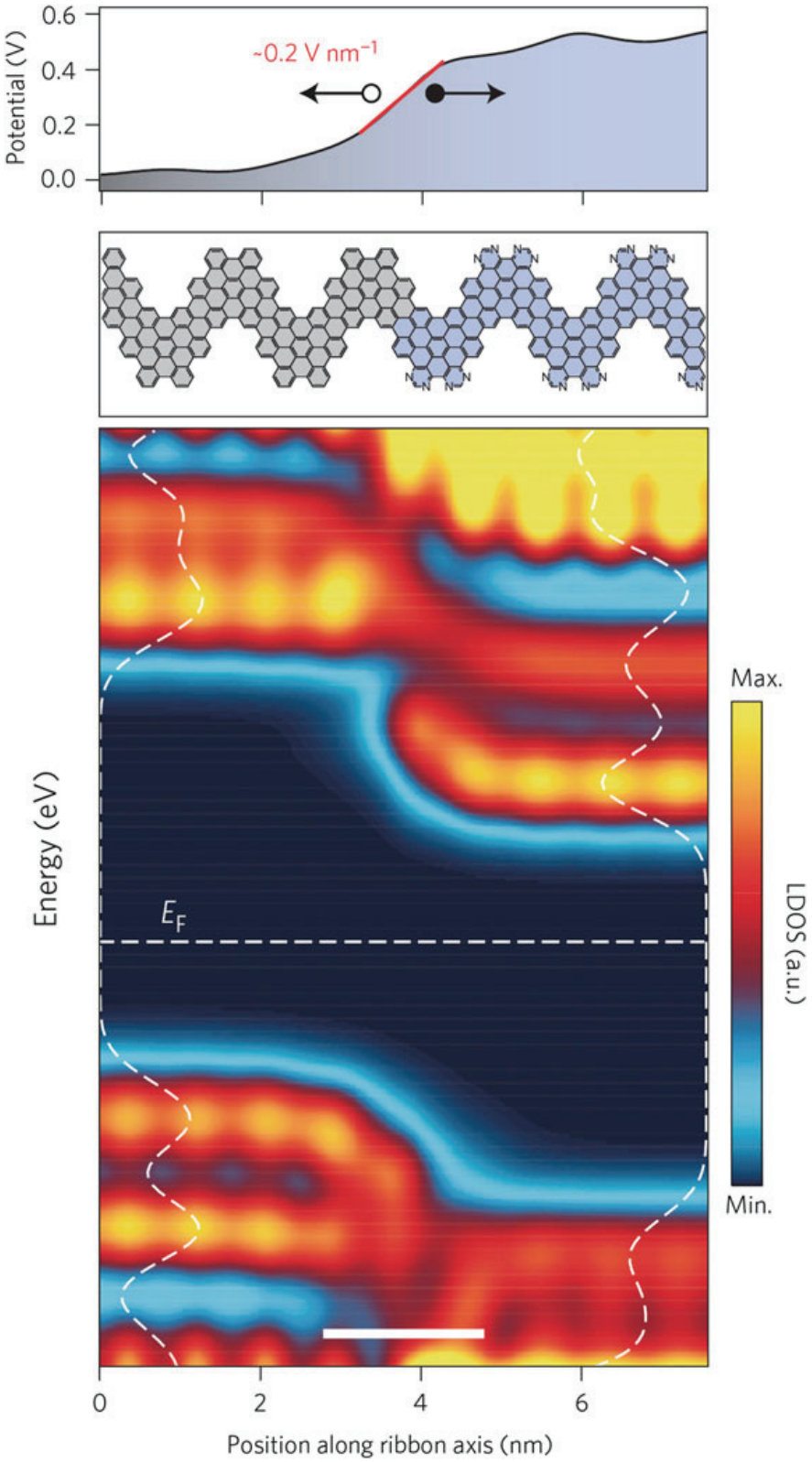

Fig. 12 Copolymerization of phenyl- and pyrimidyl-substituted monomers on Au(111), leading to p-n junctions of chevron-type GNRs. Reproduced from [24]. Copyright (2014) Nature Publishing Group

show that the interface is very sharp and that band bending is only 2 nm wide in its spatial extension (Fig. 12).

A different approach for synthesis of good conducting molecular wires is based on alternating donor–acceptor chains [26]. The coupling of donor and acceptor units lowers the HOMO–LUMO gap significantly. We prepared and polymerized bis(5-bromo-2-thienyl)-benzobis(1,2,5-thiadiazole) as the donor–acceptor–donor (DAD) monomer (Fig. 13) to obtain highly conducting, yet flexible, molecular wires [27]. The benzobis(thiadiazole) groups function as acceptor units, connected via bithiophene units formed during Ullmann-type on-surface coupling that act as donor moieties. Due to nature of the connecting C–C single bond, and in strong contrast to the stiff GNRs, the resulting conjugated donor–acceptor polymer wires are highly flexible, which enables characterization of their conductance using pulling experiments. This flexibility leads to closed structures (i.e., highly ordered rings) that are composed of only very few molecular building blocks and exhibit rather small diameters that reflect the high curvature angles that can be achieved. Specifically, $(DAD)_6$ rings (the most abundant closed structure, containing six DAD monomers) with a curvature radius of about 13.9 ± 0.2 Å and even $(DAD)_5$ rings with a radius of only 11.5 ± 0.2 Å have been found [27]. These structures indicate the high degree of conformational flexibility that can be achieved in such structures.

DAD monomers and DAD_n oligomers show a very homogeneous contrast (i.e., apparent height) in constant-current STM images (Fig. 13). Detailed information about their electronic states, in particular about the spatial distribution of these states within the molecules, can be obtained by dI/dV conductance spectroscopy

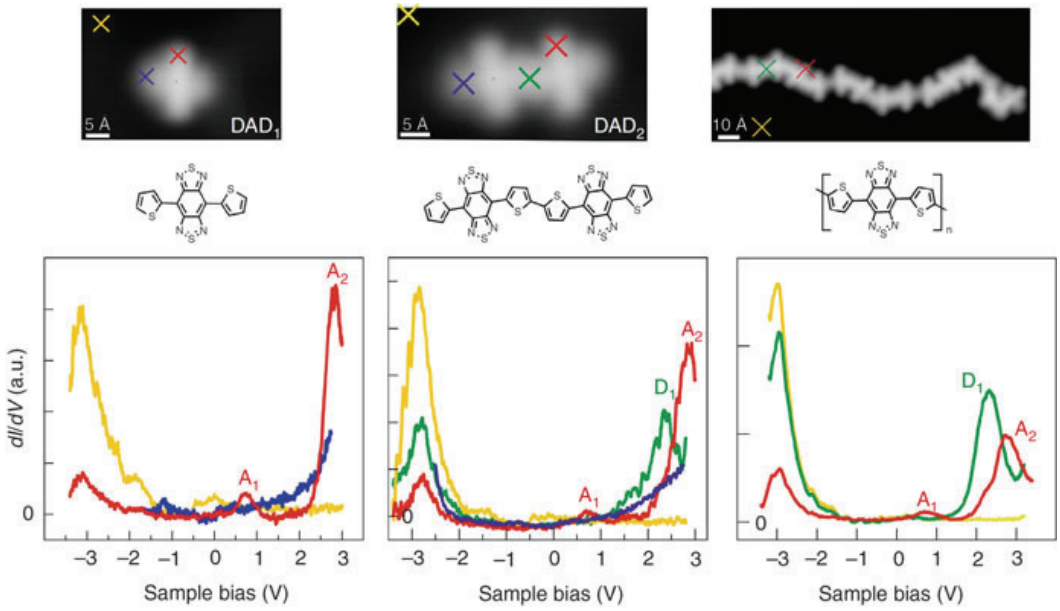

Fig. 13 Flexible wires based on alternating donor–acceptor polymers prepared by on-surface polymerization on Au(111) [27]

(at the bottom of Fig. 13), which probes the LDOS. Different unoccupied states can be identified there (all being in the range of positive bias voltages as this refers to the sample potential), named A_1, A_2, and D_1 (Fig. 13). The first two are exclusively found on the acceptor groups of the DAD_n oligomers, whereas the latter is only present on the donor groups, a finding that is valid for various lengths of chain without any significant energy shift. Hence, no efficient electron delocalization takes place for these states, otherwise they would smear out over the molecular structure and could not be as clearly distinguished on different positions along the molecular chain as reported by dI/dV maps over the oligomers [27]. Hence, the characteristic electronic states of donor and acceptor groups within an oligomer adsorbed on an Au(111) surface can be identified in terms of their spatial position and electronic energy for different oligomer lengths.

Note that the donor state D_1 is spatially located at the site of the bithiophene within the oligomer, but no feature is visible in the dI/dV spectra at this energy position at the thiophene site for the DAD monomer or at the chain terminus. The D_1 state is therefore clearly related to the linking of two thiophenes to a bithiophene unit, which is the actual donor moiety in the DAD oligomer [27]. Such an effect on the optoelectronic properties (via the energy positions of electronic states) with increasing chain length is well established in the field of π-conjugated oligomers.

5 Conductance of Molecular Wires

The conductance (G) of a molecular wire of length d decays exponentially and can be described by $G(d) = Go\ \mathrm{e}^{-\beta \mathrm{d}}$, where Go is the contact conductance and β is the inverse decay length. The inverse decay length depends on the position of the HOMO and LUMO relative to the Fermi level E_F as well as on their energy gap (E_g) and on the effective mass of the electron in the tunneling junction. Large E_g leads to high β values and, consequently, to low junction conductance, for instance for alkane chains. If the molecule in the junction exhibits electronic states that are located close to the Fermi level, another transport regime is active. In such a case, β becomes very small, for example when d-states of an organometallic compound or π-states of a conjugated organic molecule are available. Consequently, a pseudoballistic transport regime with $G < 2\mathrm{e}^2/h$ (i.e., the quantum of conductance) occurs because the electronic structure of the molecular wire differs from that of the metallic electrodes.

To measure the conductance of a single molecule, it can be lifted off the surface by controlled STM pulling (Fig. 14) [28]. One end of the molecular chain is attached to the tip and the other to the (metallic) surface. Before and after a pulling experiment, the molecular chain can be characterized by imaging and spectroscopy. While the tip is retracted, the effective transport length through the molecular chain is modified, because the current is only passing through the part of the molecule that does not interact with the surface. If the molecule is successfully lifted from the

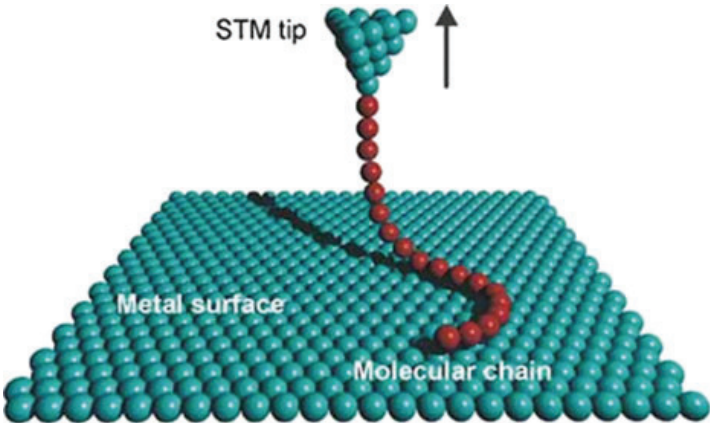

Fig. 14 In situ characterization of molecular chains, prepared by on-surface polymerization, by pulling experiments, which provide direct access to current (conductance) versus distance (chain length) curves at the single-molecule level [28]

surface, a smaller slope of the STM current signal $I(z)$ (i.e., higher conductance) than for the vacuum junction is measured during pulling.

Poly(9,9-dimethylfluorene) prepared by on-surface polymerization from dibromoterfluorene (DBTF) monomers was the first molecular wire studied using STM pulling experiments [28]. The high mobility of (activated) monomers allows formation of very long and well-defined polyfluorene chains on the Au(111) surface. Defect-free polymers with lengths exceeding 100 nm have been observed. These oligomers are highly flexible and the polyfluorene chains can be strongly curved during STM manipulation experiments.

To pull a polyfluorene chain from the surface, the tip is approached at the terminus of the chain. When contact is established, the tip is retracted while the current is being measured (Fig. 15). The current decays exponentially and regular oscillations appear in the conductance trace. These oscillations are attributed to fluorene units, which are lifted one-by-one from the surface, as shown by subsequent measurement of the same system by atomic force microscopy (AFM) [29]. The inverse decay rate is 0.38 $Å^{-1}$ for a bias voltage of 100 mV, in good agreement with theory [28].

To study the influence of molecular orbitals on transport we studied the pristine GNRs mentioned above [20]. Scanning tunneling spectroscopy showed that the HOMO and LUMO are delocalized along the edges of the GNR. We performed STM pulling experiments on these ribbons but with varied applied bias voltage. This means that we retracted the STM tip to −10 Å and then increased the bias voltage to the value of interest. We found inverse decay length values of around 0.45 $Å^{-1}$ in the HOMO–LUMO gap.

If the bias voltage is increased so that the HOMO or LUMO participate in charge transport, the inverse decay length decreases to values as low as 0.1 $Å^{-1}$ (Fig. 16). Nevertheless, no ballistic transport ($\beta = 0$ $Å^{-1}$) is achieved, as predicted by theory for flat GNRs [20], which we explain by the curvature of the ribbons during pulling experiments. The nonplanar conformation modifies the electronic structure and perturbs electronic delocalization along the molecule.

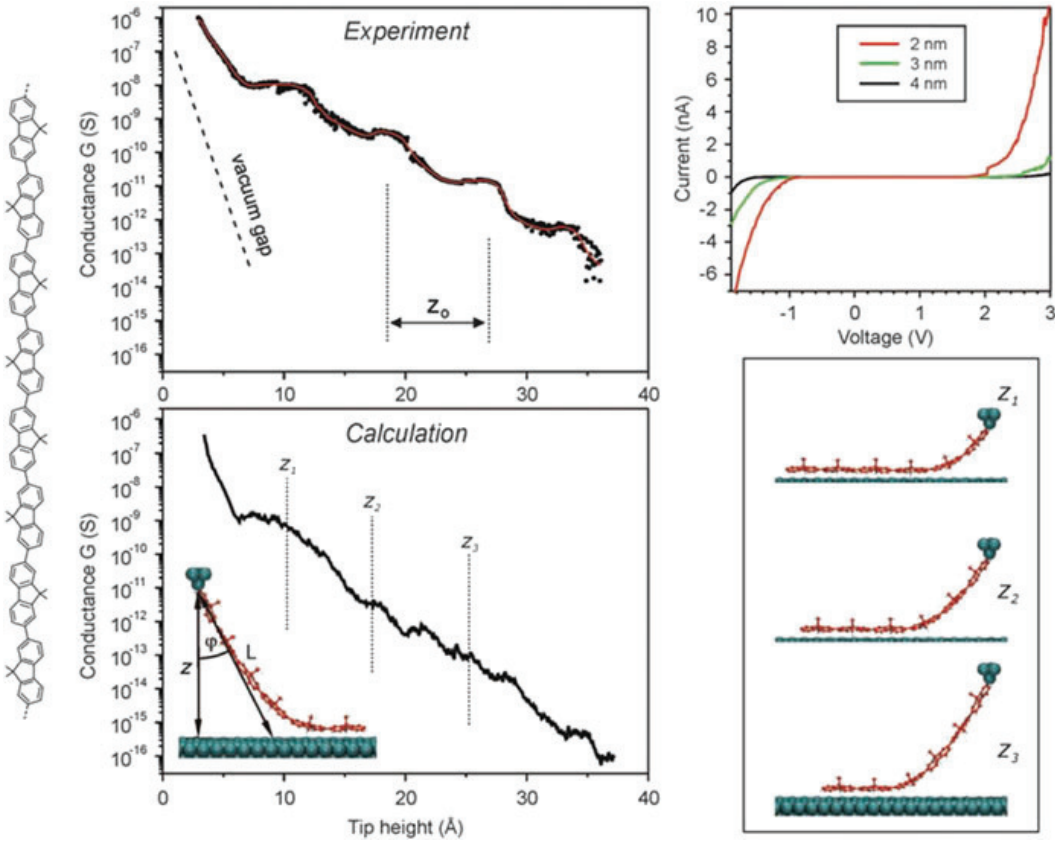

Fig. 15 Experimental and calculated conductance of an individual poly(9,9-dimethylfluorene) chain pulled off an Au(111) surface. The chemical structure of the oligomer is shown on the *left*. Reproduced from [28]

Conjugated polymer chains based on alternating donor and acceptor units (see Fig. 13) combine the high flexibility of polyfluorene chains with the inherent conductivity of GNRs. STM pulling experiments show an inverse decay length of 0.21 $Å^{-1}$ for bias voltages between −100 mV and 100 mV [27], being only weakly influenced by the applied bias voltage. This value is very low considering that these alternating donor–acceptor polymers do not have delocalized states along the molecular chain.

Direct comparison of the inverse decay lengths β, reflecting the electrical conductance, revealed a variety of values for different molecular structures [27]. Typical β values are 0.38 $Å^{-1}$ for polyfluorene (see Fig. 15) and about 0.4 $Å^{-1}$ for GNRs (see Fig. 16); polyanthracene is a rather bad conductor with a β value of about 0.8 $Å^{-1}$ as a result of its twisted structure. The smallest value of 0.21 $Å^{-1}$, and therefore best conductance, is found for the DAD_n oligomers. It should be noted that a homogeneous polymer consisting only of thiophene units (i.e., the donor groups in DAD chains) exhibits a clearly reduced conductance as compared with DAD_n oligomers [27]. Hence, it is the combination of alternating donor and acceptor groups that gives good conductance values, in combination with the molecular flexibility.

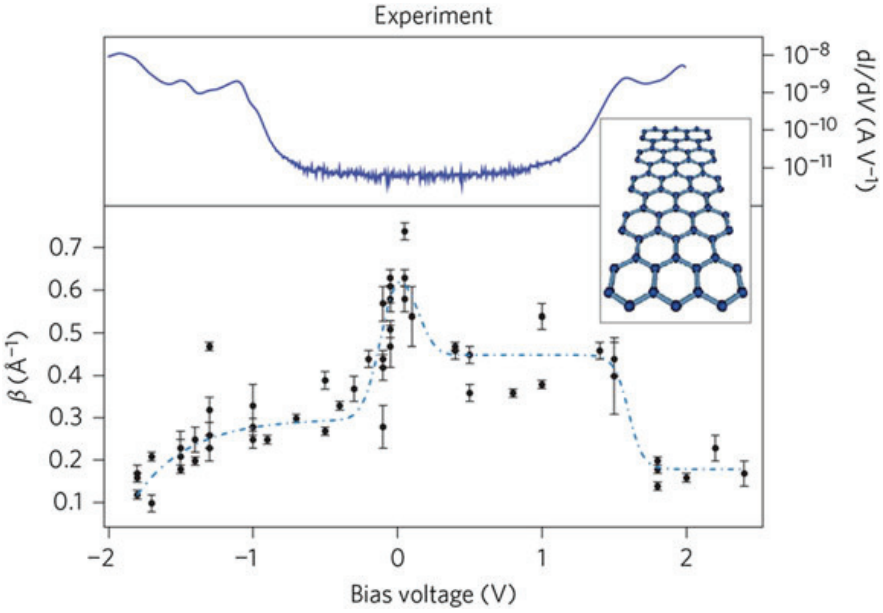

Fig. 16 Inverse decay lengths from various $N = 7$ GNRs (shown in the *inset*) for different bias values during a pulling experiment. Reproduced from [20]

6 Two-Dimensional Networks

So far we have discussed the on-surface growth of 1D structures. By increasing the number of halogen atoms (i.e., the number of reactive sites), branched structures and ideally 2D networks can be fabricated on the surface. In our initial work, porphyrin molecules were equipped with one, two, and four bromine atoms [7]. Depending on the number of bromine atoms, dimers, chains, or 2D networks were observed after heating the Au(111) substrate and activating the monomers (Fig. 17).

Whereas Ullmann-type homocoupling connects identical (het)aryl halides, the condensation of amine and aldehydes allows coupling of two different (orthogonal) reaction partners and the formed imines are typically too labile to be deposited directly onto a metal substrate by evaporation. Imine formation has been demonstrated by evaporating a star-shaped trifunctional salicyl aldehyde (1,3,5-tris [(5-*tert*-butyl-3-formyl-4-hydroxyphenyl)ethynyl]benzene) and octylamine onto Au(111) at room temperature [30]. Subsequently, the substrate was annealed at temperatures between 300 K and 400 K to trigger imine condensation and desorb the formed water and unreacted octylamine. The generated trisimine product self-assembles on the surface, either in interdigitating row-like or hexagonal honeycomb structures (Fig. 18).

After optimizing deposition of the two reactants and the conditions for imine formation, the authors employed a bifunctional amine, such as hexamethylenediamine, to perform a formal A3 + B2 polycondensation and generate covalent polymeric networks on the surface (Fig. 18, bottom) [31]. Because of

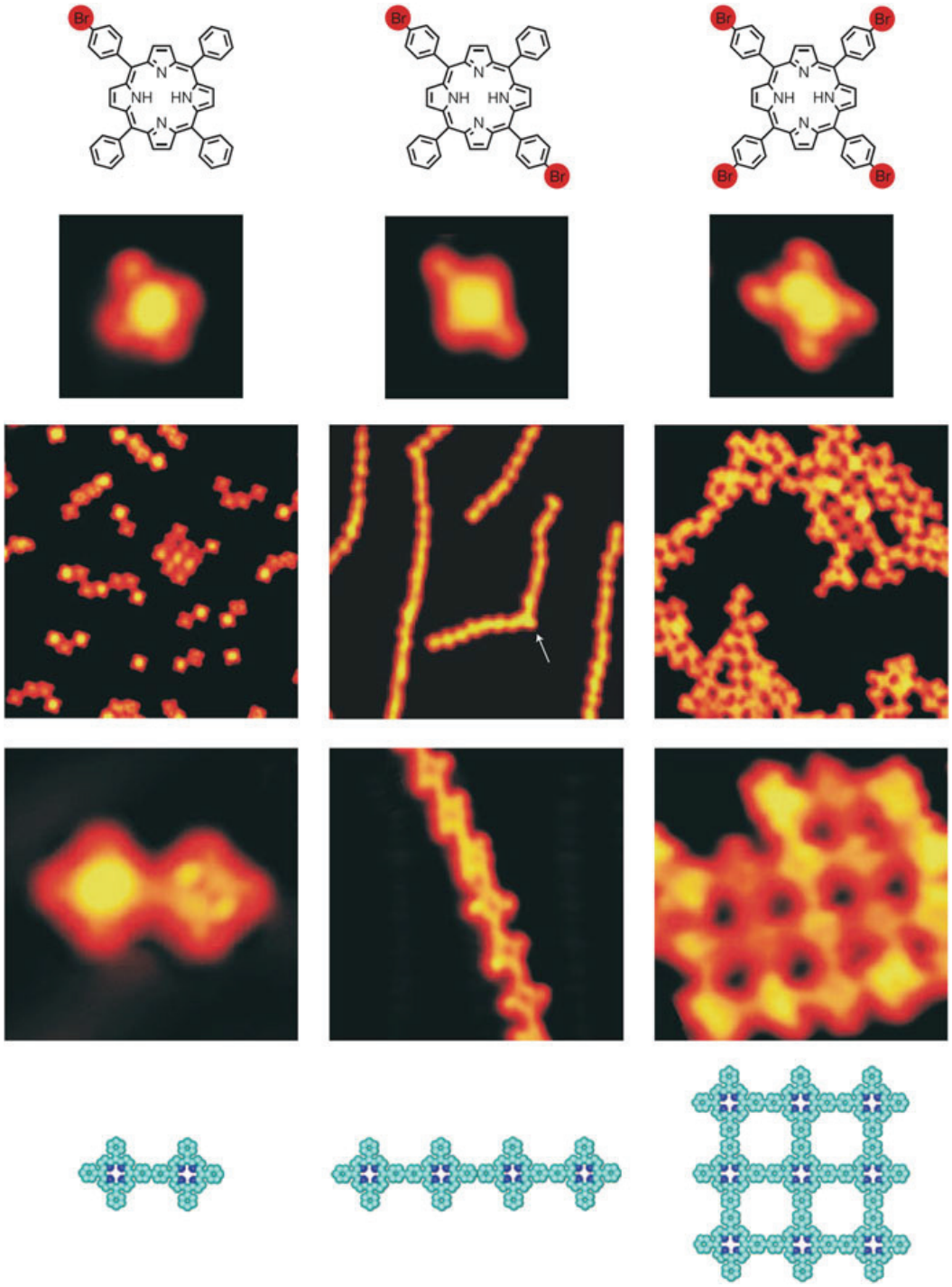

Fig. 17 On-surface polymerization of porphyrins equipped with one, two, and four bromine atoms gives rise to dimers (*left*), 1D chains (*center*), and 2D networks (*right*). Reproduced from [7]

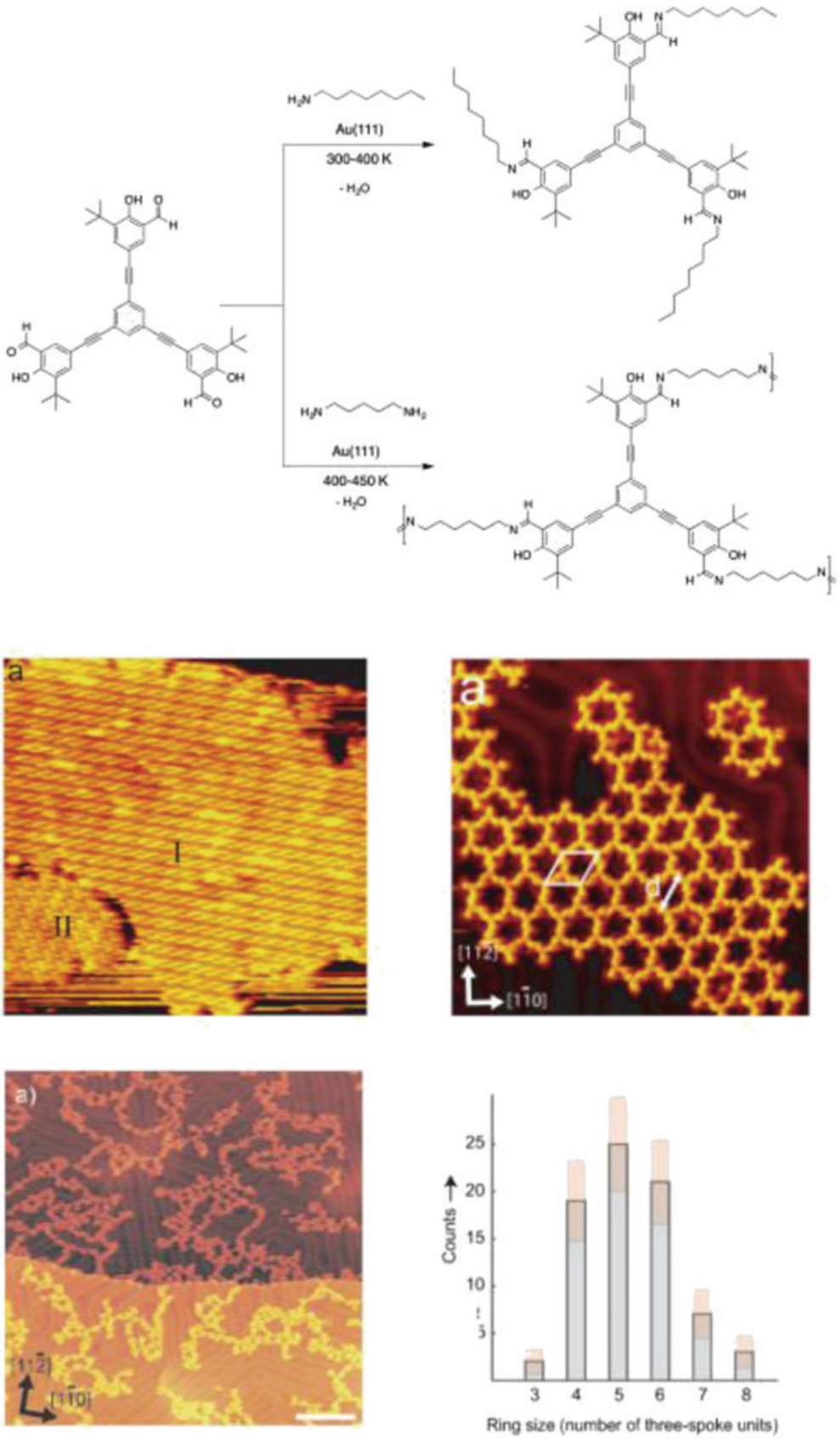

Fig. 18 Reaction of a trifunctional aldehyde with mono- and bifunctional amines on Au(111) (*top*) can lead to formation of trisimines self-assembled in rows or honeycombs (*middle*) and polyimine

the flexible structure of the diamine linker, the formed polymer network is structurally ill-defined, as exemplified by the various ring sizes formed (Fig. 18, bottom).

Although imine bonds are reversible covalent bonds, enabling defect-healing [32], in the above example the dynamic character could not be exploited, presumably because of the non-equilibrating conditions. Exploiting boroxine formation by reversible boronic acid trimerization under equilibrating conditions, Lackinger and coworkers were able to grow extended hexagonal networks (2D COFs) from 1,4-phenylenebisboronic acid in a humid atmosphere [33]. Shortly thereafter, a similar effect was shown during network formation of the extended homologue 1,4′-diphenylbisboronic acid, where equilibration was induced by intentional addition of water [34].

These two examples show that reversible connectivities allow the growth of extended 2D networks; however, the types of dynamic covalent bonds, which allow for exchange under mild conditions, are rather limited. In the context of benzene-based structures (i.e., graphene and porous phenylene networks), equilibration of aryl–aryl connections cannot typically be achieved and, hence, network formation is solely kinetically controlled.

7 Optimizing the Polymerization Process

To improve the 2D polymerization process in order to increase the size and quality of the network under kinetically controlled conditions (i.e., during C–C bond formation), the monomer concentration and reactivity are of utmost importance. Given a specific dosage/coverage, the local concentration relates to the mobility of the monomers, which is dependent on adsorbate–surface interactions and temperature. A detailed study has been carried out by the Lackinger group, showing that low surface temperatures typically favor open pores, which is explained by decreased monomer mobility on the substrate [35]. With an increase in temperature fewer open pores are found, yet increasing the temperature too far induces defects in the network (Fig. 19).

In addition, the influence of molecular flux has been studied by heating the sample to the activation temperature during deposition of monomers. Although very low deposition rates reduce the number of open pores, they also lead to formation of more pentagonal and tetragonal pores, indicating premature ring closure in the absence of new monomers. Higher deposition rates did not have a significant effect in experiments in which deposition and activation were conducted separately. Interestingly, at around 200°C or higher the authors found no difference between using BIB and tetra(*p*-bromophenyl)-quaterphenyl (TBQ), formed after initial iodine cleavage of BIB and subsequent dimerization.

Fig. 18 (continued) networks (*bottom*), respectively. Reproduced in part from [30, 31]. Copyright (2008) American Chemical Society and by Wiley-VCH, respectively

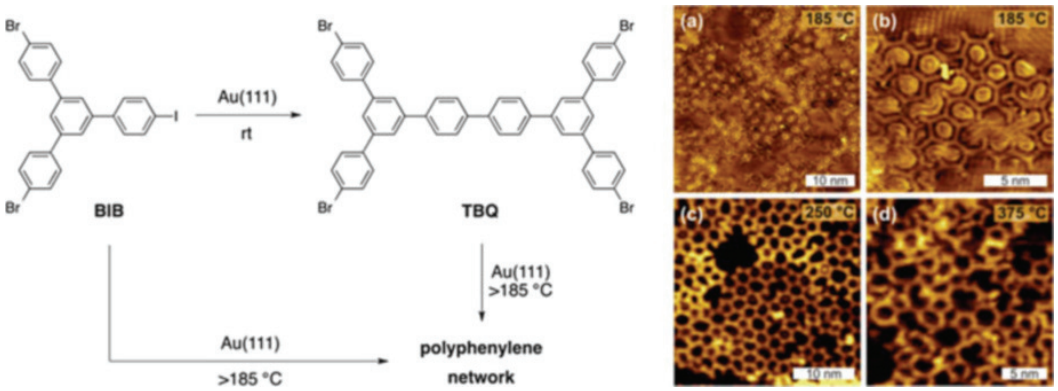

Fig. 19 Influence of the temperature of the Au(111) surface on network formation during deposition of 1,3-bis(*p*-bromophenyl)-5-(*p*-iodophenyl)benzene (BIB) and subsequent 15 min annealing. Reproduced in part from [35]. Copyright (2014) American Chemical Society

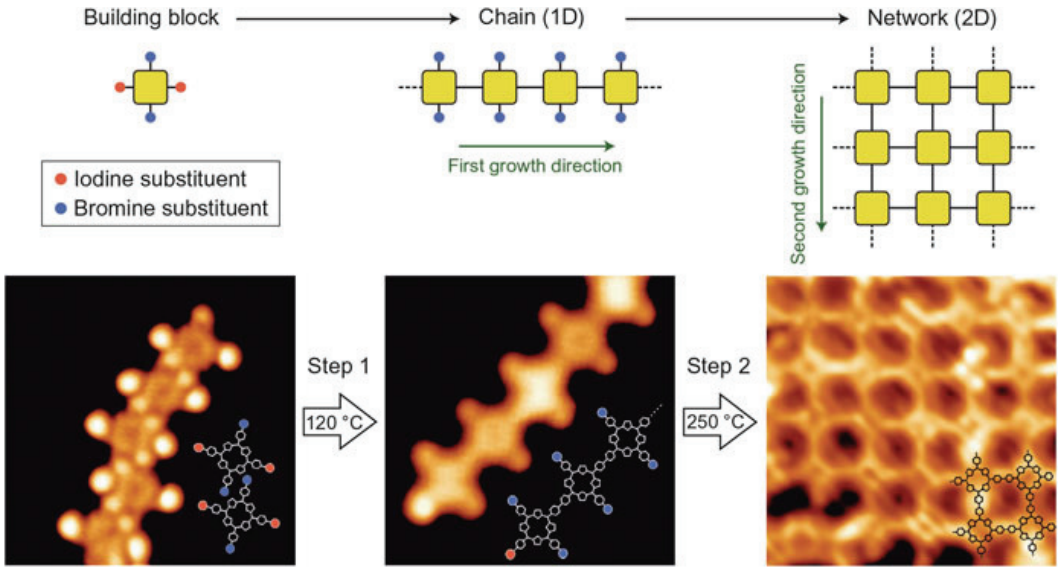

Fig. 20 Hierarchical growth of rectangular porphyrin networks by sequential activation of porphyrin monomers, in which cleavage of the iodine substituents leads to initial formation of chains, which are subsequently connected after bromine dissociation. Reproduced from [36]

Prior to these experiments, sequential activation of C–I and C–Br bonds had been used to control the 2D growth of porphyrin networks [36]. The approach is based on the different halogen–carbon bond dissociation energies (i.e., 272 kJ/mol in the case of phenyl iodide and 336 kJ/mol for phenyl bromide), which lead to different activation temperatures. In other words, monomer building blocks equipped with iodine and bromine substituents have two different activation temperatures, which enables polymerization to take place first at the cleaved iodine sites and subsequently at the cleaved bromine sites. We chose porphyrin building blocks because their fourfold symmetry allows attachment of two iodine and two bromine atoms in orthogonal directions (Fig. 20). The initial heating step to 390 K activates only the iodine sites of the porphyrin building block. The reactive sites are

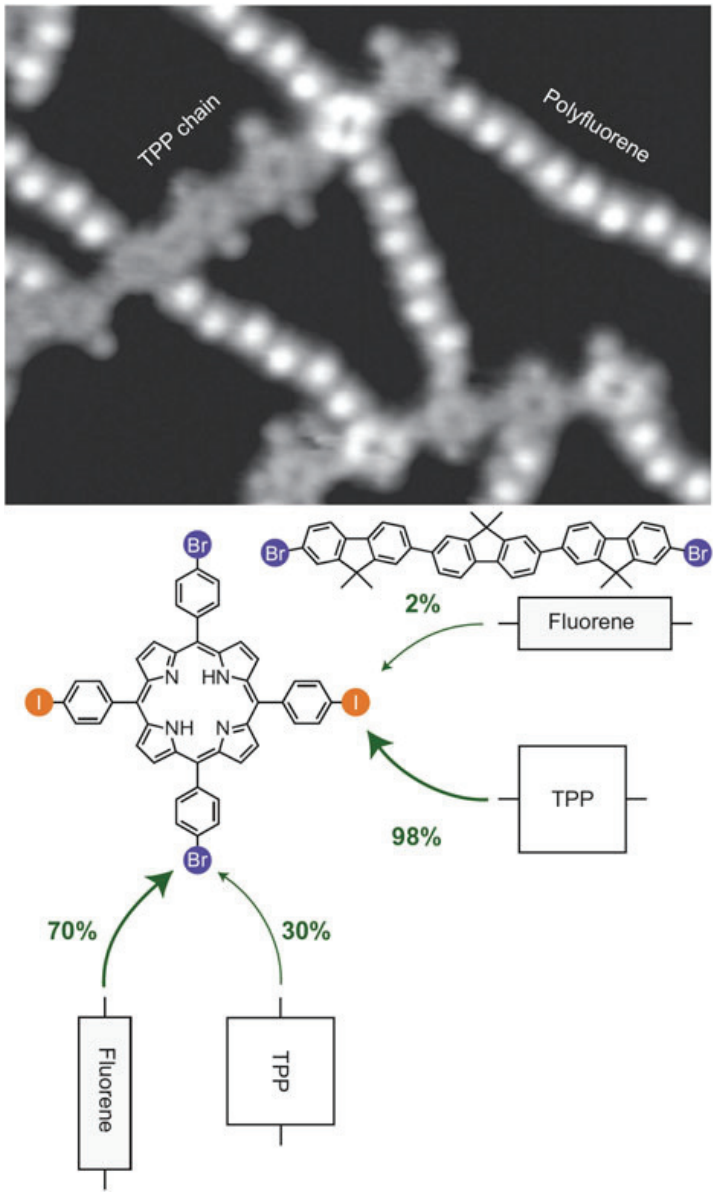

Fig. 21 Coupling selectivities observed in copolymerization using sequential activation. Reproduced from [36]

in a *trans* relationship, which leads to formation of 1D porphyrin chains. Subsequently, heating to 470 K activates orthogonal bromine sites and the porphyrin chains are connected to yield 2D networks (Fig. 20). The size and quality of the 2D porphyrin networks is higher when the chains are polymerized first (compared with 2D network formation in one step only; see Fig. 17). Although polymerization of the porphyrin chains is not reversible, it leads to preorganization of the reactive sites after bromine dissociation, and this zipper effect facilitates network formation.

Note that the fourfold symmetry of the porphyrin building blocks is ideally suited for two orthogonal growth directions.

This sequential activation technique could also be used to connect different monomer building blocks. For example, *trans*-dibromo-diiodo-porphyrin monomers were mixed with dibromoterfluorene (DBTF; see Fig. 21) and both species deposited onto the surface intact (i.e., not activated). On raising the temperature to 520 K, two reactions take place sequentially: First, only iodine atoms are cleaved and porphyrin chains are exclusively created. Then, the bromine sites are activated and DBTF forms polyfluorene chains, which attach to the porphyrins. Note that both molecular monomers are present on the surface during the entire procedure. Hence, a heterogeneous network can be formed based, on the one hand, on sequential activation and, on the other, on the relative chemoselectivities of the activated monomer building blocks (Fig. 21).

8 Outlook

Over the past decade, a joint effort by synthetic chemists and surface physicists has led to the development of on-surface synthesis, which allows polymers of various types and topologies to be prepared directly on an atomically defined surface under controlled (UHV) conditions. The growing body of work has contributed to our fundamental understanding of chemical surface reactivity and enabled preparation of a large potpourri of nanostructures, such as GNRs and nanosheets of various composition, as interesting materials for emerging applications. Although much progress has been made, several challenges remain at least partially open: (1) the degree of structure perfection utilizing reversible covalent reactions, (2) preparation of specific heterostructures involving regioselective doping and copolymers, (3) compatibility with catalytically inactive surfaces, and (4) potential transfer of reaction products. In particular, with regard to benzene-derived graphene-like structures, such as GNRs and (nano)graphene, the future will witness a continued evolution of bottom-up chemical methods and integration of these functional nanomaterials – the topic of this particular volume – into electronic devices and other applications.

References

1. Nacci C, Hecht S, Grill L (2016) The emergence of covalent on-surface polymerization. In: Gourdon A (ed) On-surface synthesis. Springer, Switzerland, pp 1–21
2. Hla S-W, Bartels L, Meyer G, Rieder KH (2000) Inducing all steps of a chemical reaction with the scanning tunneling microscope tip: towards single molecule engineering. Phys Rev Lett 85:2777–2780
3. Ullmann F, Bielecki J (1901) Über Synthesen in der Biphenylreihe. Chem Ber 34:2174–2185

4. Bieri M, Nguyen M-T, Gröning O, Cai J, Treier M, Aït-Mansour K, Ruffieux P, Pignedoli CA, Passerone D, Kastler M, Müllen K, Fasel R (2010) Two-dimensional polymer formation on surfaces: insight into the roles of precursor mobility and reactivity. J Am Chem Soc 132:16669–16676
5. Saywell A, Schwarz J, Hecht S, Grill L (2012) Polymerization on stepped surfaces: alignment of polymers and identification of catalytic sites. Angew Chem Int Ed 51:5096–5100
6. Cram D, Hendrickson J, Hammond G (1970) Organic chemistry, 3rd edn. McGraw-Hill, New York
7. Grill L, Dyer M, Lafferentz L, Persson M, Peters MV, Hecht S (2007) Nano-architectures by covalent assembly of molecular building blocks. Nat Nanotechnol 2:687–691
8. McCarthy GS, Weiss PS (2004) Formation and manipulation of protopolymer chains. J Am Chem Soc 126:16772–16776
9. Lipton-Duffin JA, Ivasenko O, Perepichka DF, Rosei F (2009) Synthesis of polyphenylene molecular wires by surface-confined polymerization. Small 5:592–597
10. Zhang H, Lin H, Sun K, Chen L, Zagranyarski Y, Aghdassi N, Duhm S, Li Q, Zhong D, Li Y, Müllen K, Fuchs H, Chi L (2015) On-surface synthesis of rylene-type graphene nanoribbons. J Am Chem Soc 137:4022–4025
11. Scholl R, Seer C (1912) Abspaltung aromatisch gebundenen Wasserstoffs und Verknüpfung aromatischer Kerne durch Aluminiumchlorid. Justus Liebigs Ann Chem 394:111–177
12. Cai J, Ruffieux P, Jaafar R, Bieri M, Braun T, Blankenburg S, Muoth M, Seitsonen AP, Saleh M, Feng X, Müllen K, Fasel R (2010) Atomically precise bottom-up fabrication of graphene nanoribbons. Nature 466:470–473
13. Koch M (2013) Growth and characterization of single molecular wires on metal surfaces. Dissertation, Freie Universität Berlin
14. Ruffieux P, Wang S, Yang B, Sánchez-Sánchez C, Liu J, Dienel T, Talirz L, Shinde P, Pignedoli CA, Passerone D, Dumslaff T, Feng X, Müllen K, Fasel R (2016) On-surface synthesis of graphene nanoribbons with zigzag edge topology. Nature 531:489–492
15. Soe W-H, Wong HS, Manzano C, Grisolia M, Hliwa M, Feng X, Müllen K, Joachim C (2012) Mapping the excited states of single hexa-peri-benzocoronene oligomers. ACS Nano 6:3230–3235
16. Koch M, Gille M, Viertel A, Hecht S, Grill L (2014) Substrate-controlled linking of molecular building blocks: Au(111) vs. Cu(111). Surf Sci 627:70–74
17. Walch H, Gutzler R, Sirtl T, Eder G, Lackinger M (2010) Material- and orientation-dependent reactivity for heterogeneously catalyzed carbon−bromine bond homolysis. J Phys Chem C 114:12604–12609
18. Kittelmann M, Rahe P, Nimmrich M, Hauke CM, Gourdon A, Kühnle A (2011) On-surface covalent linking of organic building blocks on a bulk insulator. ACS Nano 5:8420–8425
19. Villagomez CJ, Sasaki T, Tour JM, Grill L (2010) Bottom-up assembly of molecular wagons on a surface. J Am Chem Soc 132:16848–16854
20. Koch M, Ample F, Joachim C, Grill L (2012) Voltage-dependent conductance of a single graphene nanoribbon. Nat Nanotechnol 7:713–717
21. Söde H, Talirz L, Gröning O, Pignedoli CA, Berger R, Feng X, Müllen K, Fasel R, Ruffieux P (2015) Electronic band dispersion of graphene nanoribbons via Fourier-transformed scanning tunneling spectroscopy. Phys Rev B 91:045429
22. Bronner C, Leyssner F, Stremlau S, Utecht M, Saalfrank P, Klamroth T, Tegeder P (2012) Electronic structure of a subnanometer wide bottom-up fabricated graphene nanoribbon: end states, band gap, and dispersion. Phys Rev B 86:085444
23. Linden S, Zhong D, Timmer A, Aghdassi N, Franke JH, Zhang H, Feng X, Müllen K, Fuchs H, Chi L, Zacharias H (2012) Electronic structure of spatially aligned graphene nanoribbons on Au(788). Phys Rev Lett 108:216801
24. Cai J, Pignedoli CA, Talirz L, Ruffieux P, Söde H, Linag L, Meunier V, Berger R, Li R, Feng X, Müllen K, Fasel R (2014) Graphene nanoribbon heterojunctions. Nat Nanotechnol 9:896–900

25. Bronner C, Stremlau S, Gille M, Braußе F, Haase A, Hecht S, Tegeder P (2013) Aligning the band gap of graphene nanoribbons by monomer doping. Angew Chem Int Ed 52:4422–4425
26. Mullekom HAMV, Vekemans JAJM, Havinga EE, Meijer EW (2000) Developments in the chemistry and band gap engineering of donor-acceptor substituted conjugated polymers. Mater Sci Eng 32:1–40
27. Nacci C, Ample F, Bléger D, Hecht S, Joachim C, Grill L (2015) Conductance of a single flexible molecular wire composed of alternating donor and acceptor units. Nat Commun 6:7397
28. Lafferentz L, Ample F, Yu H, Hecht S, Joachim C, Grill L (2009) Conductance of a single conjugated polymer as a continuous function of its length. Science 323:1193–1197
29. Kawai S, Koch M, Gnecco E, Sadeghi A, Pawlak R, Glatzel T, Schwarz J, Goedecker S, Hecht S, Baratoff A, Grill L, Meyer E (2014) Quantifying the atomic-level mechanics of single long physisorbed molecular chains. Proc Natl Acad Sci 111:3968–3972
30. Weigelt S, Bombis C, Busse C, Knudsen MM, Gothelf KV, Lægsgaard E, Besenbacher F, Linderoth TR (2008) Molecular self-assembly from building blocks synthesized on a surface in ultrahigh vacuum: kinetic control and topo-chemical reactions. ACS Nano 2:651–660
31. Weigelt S, Bombis C, Busse C, Knudsen MM, Gothelf KV, Lægsgaard E, Besenbacher F, Linderoth TR (2008) Surface synthesis of 2D branched polymer nanostructures. Angew Chem Int Ed 47:4406–4410
32. Belowich ME, Stoddart JF (2012) Dynamic imine chemistry. Chem Soc Rev 41:2003–2024
33. Dienstmaier JF, Gigler AM, Goetz AJ, Knochel P, Bein T, Lyapin A, Reichlmaier S, Heckl WM, Lackinger M (2011) Synthesis of well-ordered COF monolayers: surface growth of nanocrystalline precursors versus direct on-surface polycondensation. ACS Nano 12:9737–9745
34. Guan C-Z, Wang D, Wan L-J (2012) Construction and repair of highly ordered 2D covalent networks by chemical equilibrium regulation. Chem Commun 48:2943–2945
35. Eichhorn J, Nieckarz D, Ochs O, Samantha S, Schmittel M, Szabelski PJ, Lackinger M (2014) On-surface ullmann coupling: the influence of kinetic reaction parameters on the morphology and quality of covalent networks. ACS Nano 8:7880–7889
36. Lafferentz L, Eberhardt V, Dri C, Africh C, Comelli G, Esch F, Hecht S, Grill L (2012) Controlling on-surface polymerization by hierarchical and substrate-directed growth. Nat Chem 4:215–220